Available online at www.sciencedirect.com
SCIENCE DIRECT®
International Journal of Thermal Sciences 45 (2006) 70–85
International Journal of Thermal Sciences
www.elsevier.com/locate/ijts

A systems CFD model of a packed bed high temperature gas-cooled nuclear reactor ☆

C.G. du Toit [a,*], P.G. Rousseau [a], G.P. Greyvenstein [a], W.A. Landman [b]

[a] *School of Mechanical and Materials Engineering, North-West University, Private Bag X6001, Potchefstroom 2520, South Africa*
[b] *M-Tech Industrial, PO Box 19855, Noordbrug 2522, South Africa*

Received 1 September 2004; received in revised form 25 April 2005; accepted 30 April 2005

Available online 15 June 2005

Abstract

The theoretical basis and conceptual formulation of a comprehensive reactor model to simulate the thermal-fluid phenomena of the PBMR reactor core and core structures is given. Through a rigorous analysis the fundamental equations are recast in a form that is suitable for incorporation in a systems CFD code. The formulation of the equations results in a collection of one-dimensional elements (models) that can be used to construct a comprehensive multi-dimensional network model of the reactor. The elements account for the pressure drop through the reactor; the convective heat transport by the gas; the convection heat transfer between the gas and the solids; the radiative, contact and convection heat transfer between the pebbles and the heat conduction in the pebbles. Results from the numerical model are compared with that of experiments conducted on the SANA facility covering a range of temperatures as well as two different fluids and different heating configurations. The good comparison obtained between the simulated and measured results show that the systems CFD approach sufficiently accounts for all of the important phenomena encountered in the quasi-steady natural convection driven flows that will prevail after critical events in a reactor. The fact that the computer simulation time for all of the simulations was less than three seconds on a standard notebook computer also indicates that the new model indeed achieves a fine balance between accuracy and simplicity. The new model can therefore be used with confidence and still allow quick integrated plant simulations.

Keywords: Packed bed; High temperature gas-cooled reactor; Systems CFD; Natural convection; Network model

1. Introduction

The pebble bed modular reactor (PBMR) [1] power plant is currently being developed by PBMR (Pty) Ltd in South Africa in association with ESKOM and other industrial partners. This high-temperature gas-cooled reactor (HTGR) plant is based on a three-shaft Brayton cycle with helium gas as coolant. Engineers are faced with two major challenges when carrying out the thermal-flow design of a HTGR power plant. The first challenge is to predict the performance of all the thermal-flow components of the plant such as pipes, valves, heat exchangers, turbo machines and the reactor [2]. The second challenge is to predict the performance of the integrated plant consisting of all its sub-systems. The complexity associated with the thermal-flow design of the cycle requires the use of a variety of analysis techniques and simulation tools. These range from simple one-dimensional models [3] that do not capture all the significant physical phenomena to large-scale three-dimensional CFD codes [4] that, for practical reasons, cannot simulate the entire plant as a single integrated system. System performance predictions must be done for both steady-state and transient conditions. Transient analyses are required for control studies and for studying operating procedures such as start-up, load rejection, load following and accident events.

The integration of the power conversion unit (PCU) thermal-flow analysis and core neutronics has been done

☆ A preliminary version of this paper was presented at CHT-04: An ICHMT International Symposium on Advances in Computational Heat Transfer, April 2004, G. de Vahl Davis and E. Leonardi (Eds.), CD-ROM Proceedings, ISBN 1-5670-174-2, Begell House, New York, 2004.

* Corresponding author. Tel.: +27 18 299 1322; fax: +27 18 299 1322.
E-mail address: mgicgdt@puk.ac.za (C.G. du Toit).

1290-0729/$ – see front matter © 2005 Elsevier SAS. All rights reserved.
doi:10.1016/j.ijthermalsci.2005.04.010

Nomenclature

A	area	m^2
$\vec{B}$	resistance force due to pebbles	$N{\cdot}m^{-3}$
c_p	specific heat capacity a constant pressure	$J{\cdot}kg^{-1}{\cdot}K^{-1}$
c_v	specific heat capacity at constant volume	$J{\cdot}kg^{-1}{\cdot}K^{-1}$
d	diameter	m
E	total specific energy	$J{\cdot}kg^{-1}$
e	specific internal energy	$J{\cdot}kg^{-1}$
$\vec{g}$	gravitational acceleration vector	$m{\cdot}s^{-2}$
h	specific enthalpy	$J{\cdot}kg^{-1}$
k	thermal conductivity	$W{\cdot}m^{-1}{\cdot}K^{-1}$
L	length	m
$\dot{m}$	mass flow rate	$kg{\cdot}s^{-1}$
$\vec{n}$	unit vector normal to surface	
p	pressure	$N{\cdot}m^{-2}$
	static pressure	$N{\cdot}m^{-2}$
$\vec{q}$	heat flux vector	$W{\cdot}m^{-2}$
q'''	heat generated per unit volume	$W{\cdot}m^{-3}$
R	radius	m
r	radial coordinate	m
T	temperature	K
u	velocity component	$m{\cdot}s^{-1}$
$\vec{V}$	velocity vector	$m{\cdot}s^{-1}$
$\overline{V}$	volume of control volume	m^3
z	axial coordinate	m

Greek symbols

ε	porosity	
ϵ	effectiveness	
θ	tangential coordinate	rad
μ	dynamic viscosity	
ρ	density	$kg{\cdot}m^{-3}$
$\boldsymbol{\sigma}$	stress tensor	$N{\cdot}m^{-2}$

Subscripts

b	bulk
eff	effective
e, w, n, s	east, west, north and south
f	fluid
i, o	inner, outer
o	total
p	pebble
	cell centre
r	radial direction
s	solid
z	axial direction
θ	tangential direction

successfully before for HTGR systems. Verkerk [5] coupled the Panther, Thermix-Direkt and Relap5 codes for the simulation of the pebble bed reactor for the Dutch INCOGEN and ACACIA studies. Panther was used to solve neutron diffusion equations; Thermix-Direkt took care of the core thermal-flow analysis and Relap5 of the PCU thermal-flow simulation. The SPECTRA code developed by Stempniewicz [6] is capable of analysing a whole power plant, including the reactor vessel, primary system, various control and safety systems, containment and reactor building. The code essentially consists of a library of one-dimensional models that can be used to build up the global model of the particular case in hand. Kikstra [7] developed a model of a whole cogeneration nuclear gas turbine power plant using the code Aspen Custom Modeller. A discretised reactor model with ten axial layers was employed. The model included the pebble bed core and four axially discretised reflector layers. The heat release in the pebbles was modelled with the point kinetics approximation using six delayed precursor groups.

A prominent code that provides a suitable compromise is the thermal-flow integrated systems CFD or network simulation code Flownex [8]. Flownex allows detailed steady-state and transient thermal-flow simulations of the complete power plant, fully integrated with core neutronics and controller algorithms. Flownex currently contains a simplified model for the pebble bed nuclear reactor [9]. The purpose of the model was not to do detail reactor design, but rather to allow for the integrated simulation of the reactor together with the PCU within acceptable computer simulation times. These integrated simulations are essential for design studies of the gas pipe and equipment layout, the plant controllers and auxiliary systems such as the reactor unit cooling system (RUCS). The requirement for the existing model was therefore to provide quick results of the main flow and heat transfer phenomena in the core only, in order to obtain boundary values for the simulation of the rest of the PCU. The existing model consists of three main parts namely:

- Heat transfer and fluid flow of the gas within the core. The model is based on a discretised two-dimensional axi-symmetric frame of reference with any number of control volumes in the axial and/or radial directions. The model includes the convection heat transfer between the gas and the surface of a representative sphere in each of the control volumes. However, it only allows for the simulation of the core itself, excluding all core structures, and is based on a core layout with a central homogeneous graphite pebble region and an annular homogeneous fuel pebble region surrounding the central region. Also, it does not allow for the addition or extraction of leak flows from the inner or outer perimeter of the core and the gas inlet and outlet is assumed to be from voids at the very top and very bottom of the core.
- Heat conduction within the pebbles. Each of the core control volumes contains a representative pebble for

which the heat conduction is modelled in a one-dimensional spherical frame of reference together with the convection heat transfer between the gas and the surface of the sphere. Fuel pebbles consist of an outer graphite layer and an inner fuel matrix region, both of which can be discretised into any number of spherical 'onion ring shaped' control volumes, whilst graphite pebbles consist only of graphite which can be discretised into any number of spherical 'onion ring shaped' control volumes. This allows for the calculation of the temperature distribution within the pebbles in any region of the core. The nuclear power generated in the core is distributed within the fuel matrix region of the fuel pebbles only in the form of a source term in the heat conduction equation.
- Nuclear power and decay heat generation model is based on a zero-dimensional point-kinetics approach.

Recent developments in the design and layout of the PBMR reactor have given rise to the need for the simulation of a wider range of reactor phenomena, even within a simplified model, since these will influence the boundary values for the integrated plant simulations. The phenomena that cannot be simulated in the existing model include the following:

- The presence of a fixed central reflector column that implies that the core itself has an annular rather than a cylindrical shape.
- The addition and extraction of gas via purpose provided channels and/or leak flow paths along the inner or outer perimeters of the core.
- The simulation of heat transfer and fluid flow through porous and solid core structures surrounding the core.
- The simulation of fluid flow and heat transfer, including radiation and natural convection, in purpose provided cavities between core structures with a two-dimensional rather than one-dimensional nature.
- The ability to take into account variations in porosity throughout the core.
- The ability to specify normalised radial power distribution profiles within the different axial layers in the core.
- The ability to take heat generation that may occur in any of the core structures into account.

Fig. 1 shows a simplified section through a part of what can typically be expected in the reactor geometry. The fuel pebbles are located in the annular volume formed between the central reflector and the core structures. The gas is fed from the PCU to a ring-shaped inlet manifold. From there it flows up through vertical riser channels situated at discrete intervals around the circumference. The riser channels are intersected at the top by horizontal inlet slots that feed the gas inward and into the pebble bed at the top. Besides the riser channels and inlet slots, the core structures can also contain vertical control rod channels. The control rod channels are also situated at discrete intervals around the circumference, but alternating with the riser channels. Note that

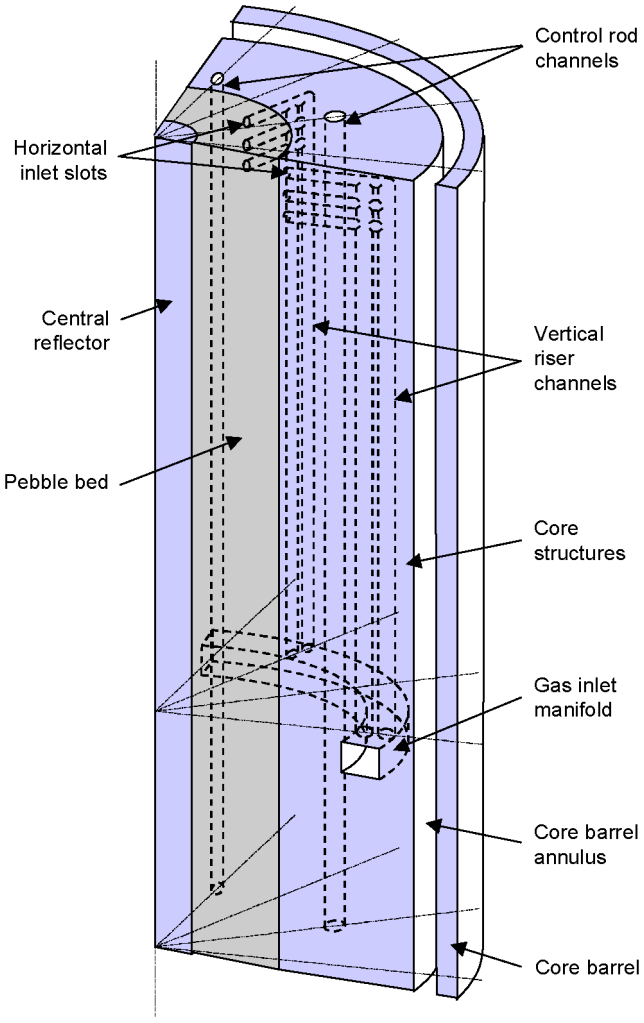

Fig. 1. Section through part of a typical reactor geometry.

the gas flowing in the riser channels does not mix with the gas contained in the control rod channels. The main core structures are typically surrounded by an annular gas-filled cavity contained within the core barrel. The core barrel in turn is contained within the reactor pressure vessel (RPV).

A need, therefore, exists for the development of a new, more comprehensive pebble bed reactor model that can still provide relatively quick integrated plant simulations, but the phenomena listed above incorporated. This paper describes the theoretical basis and formulation of the thermal-hydraulics of a more comprehensive reactor model capable of capturing the significant physical phenomena.

2. Theoretical overview

2.1. Simulation methodology

The aim of the new model is to achieve a fine balance between accuracy and simplicity and to guard against simply developing another detailed CFD code that does not allow quick integrated plant simulations. This means that the sim-

plest possible model must be derived that can sufficiently account for all of the important phenomena.

One of the first simplifications is that the model will be based on a two-dimensional axi-symmetric coordinate system rather than a full three-dimensional cylindrical coordinate system. This implies that all variations in geometry or material properties around the perimeter of the reactor will be spread evenly around the circumference to form a material with constant properties at each given height and radius. For instance, the inlet slots situated at discrete intervals around the perimeter will be represented by a material with representative unidirectional radial flow permeability. Similarly the discrete vertical control rod channels will be represented by a material with representative unidirectional axial flow permeability. The pebble bed in turn will be represented by a porous medium with multidirectional porosity rather than a unidirectional permeability. Note however, that the magnitude of the permeability or porosity may vary between control volumes in both the radial and axial directions. By employing this two-dimensional approach with representative permeability or porosity, all of the desired phenomena may be simulated, although in less detail than would be the case in a traditional CFD code. However, the reduction in the size of the required computational grid is substantial thus resulting is much faster simulation times.

The model is based on the fundamental equations for the conservation of mass, momentum and energy for compressible fluid flow, as well as the equations for the conservation of energy for the pebble and core structure solid materials. Through a rigorous analysis the equations are reduced and recast in a form that is suitable for incorporation in a network code. This formulation of the equations results in a collection of one-dimensional elements (models) and nodes (control volumes) that can be used to construct a comprehensive multi-dimensional model of the reactor. The elements account for the pressure drop through the reactor; the convective heat transport by the gas; the convection heat transfer between the gas and the solids; the radiative, contact and convection heat transfer between the pebbles and the heat conduction in the pebble and core structure materials. The numerical formulation of the equations is based on a staggered grid approach and a computationally effective segregated implicit pressure correction method [10] is employed to solve the resulting equations.

2.2. Governing equations

The governing equations for the conservation of mass, momentum and energy for the fluid will first be stated in vector form and the equations are then rewritten in terms of axi-symmetric cylindrical coordinates. Subsequently the equations for the conservation of energy in the solids will be discussed.

Fluid. The conservation equations in integral form for mass, momentum, and energy for the fluid in the pebble-bed reactor can be written as [11,12]

$$\frac{\mathrm{d}}{\mathrm{d}t}\int_{\overline{V}} \varepsilon\rho \,\mathrm{d}\overline{V} + \int_{A} \varepsilon\{\rho\vec{V}\cdot\vec{n}\}\,\mathrm{d}A = 0 \tag{1}$$

$$\frac{\mathrm{d}}{\mathrm{d}t}\int_{\overline{V}} \varepsilon\rho\vec{V}\,\mathrm{d}\overline{V} + \int_{A} \varepsilon\big\{(\vec{n}\cdot\vec{V})\rho\vec{V} - \vec{n}\boldsymbol{\sigma}\big\}\,\mathrm{d}A = \int_{\overline{V}} \varepsilon\rho\vec{g}\,\mathrm{d}\overline{V} - \int_{\overline{V}} \vec{B}\,\mathrm{d}\overline{V} \tag{2}$$

$$\frac{\mathrm{d}}{\mathrm{d}t}\int_{\overline{V}} \varepsilon\rho E\,\mathrm{d}\overline{V} + \int_{A} \varepsilon\vec{n}\cdot\{\rho E\vec{V} - \boldsymbol{\sigma}\vec{V} + \vec{q}\}\,\mathrm{d}A = \int_{\overline{V}} \big(\varepsilon\rho\vec{g}\vec{V} + q'''_{\mathrm{sf}}\big)\,\mathrm{d}\overline{V} \tag{3}$$

If it is assumed that the properties of the fluid are continuous and sufficiently differentiable, then the conservation equations in integral form (1) to (3) can be transformed into an equivalent set of partial differential equations through the divergence theorem. The pressure term in Eq. (2) is transformed according to the procedure outlined by Bey and Eigenberger [13]. The equation for the conservation of mass (1) can be expressed in axi-symmetric cylindrical coordinates as

$$\frac{\partial}{\partial t}(\varepsilon\rho) + \frac{1}{r}\frac{\partial}{\partial r}(\varepsilon\rho r u_r) + \frac{\partial}{\partial z}(\varepsilon\rho u_z) = 0 \tag{4}$$

The equation for the conservation of momentum in the radial direction can be obtained from (2) as

$$\frac{\partial}{\partial t}(\varepsilon\rho u_r) + \frac{1}{r}\frac{\partial}{\partial r}(\varepsilon\rho r u_r u_r) + \frac{\partial}{\partial z}(\varepsilon\rho u_z u_r) = -\varepsilon\frac{\partial p}{\partial r} + \frac{1}{r}\frac{\partial}{\partial r}(\varepsilon r\tau_{rr}) + \frac{\partial}{\partial z}(\varepsilon\tau_{zr}) - \frac{\varepsilon\tau_{\theta\theta}}{r} + \varepsilon\rho g_r - B_r \tag{5}$$

Extract the continuity equation (4) from (5), add and subtract the dynamic head, convert the static pressure to the total pressure [10] and transform the convective terms. This then leads to

$$\varepsilon\rho\frac{\partial u_r}{\partial t} + \varepsilon\rho u_z\left(\frac{\partial u_r}{\partial z} - \frac{\partial u_z}{\partial r}\right) = -\varepsilon\left[\frac{\rho V^2}{2T_o}\frac{\partial T_o}{\partial r} + \frac{p}{p_o}\frac{\partial p_o}{\partial r}\right] + \frac{1}{r}\frac{\partial}{\partial r}(\varepsilon r\tau_{rr}) + \frac{\partial}{\partial z}(\varepsilon\tau_{zr}) - \frac{\varepsilon\tau_{\theta\theta}}{r} + \varepsilon\rho g_r - B_r \tag{6}$$

Similarly the equation for the conservation of momentum in the axial direction can be obtained as

$$\varepsilon\rho\frac{\partial u_z}{\partial t} + \varepsilon\rho u_r\left(\frac{\partial u_z}{\partial r} - \frac{\partial u_r}{\partial z}\right) = -\varepsilon\left[\frac{\rho V^2}{2T_o}\frac{\partial T_o}{\partial z} + \frac{p}{p_o}\frac{\partial p_o}{\partial z}\right] + \frac{1}{r}\frac{\partial}{\partial r}(\varepsilon r\tau_{rz}) + \frac{\partial}{\partial z}(\varepsilon\tau_{zz}) + \varepsilon\rho g_z - B_z \tag{7}$$

The equation for the conservation of energy in terms of the total specific enthalpy can be obtained from (3) as

$$\begin{aligned}\frac{\partial}{\partial t}(\varepsilon\rho h_o)+\frac{1}{r}\frac{\partial}{\partial r}(\varepsilon r\rho h_o u_r)+\frac{\partial}{\partial z}(\varepsilon\rho h_o u_z)\\ =\varepsilon\frac{\partial p}{\partial t}+\frac{1}{r}\frac{\partial}{\partial r}\left(\varepsilon rk\frac{\partial T}{\partial r}\right)+\frac{\partial}{\partial z}\left(\varepsilon k\frac{\partial T}{\partial z}\right)\\ +\varepsilon\rho(g_r u_r+g_z u_z)+q'''_{\mathrm{sf}}+\frac{1}{r}\frac{\partial}{\partial r}\big(\varepsilon r[\tau_{rr}u_r+\tau_{rz}u_z]\big)\\ +\frac{\partial}{\partial z}\big(\varepsilon[\tau_{zr}u_r+\tau_{zz}u_z]\big)\end{aligned}\tag{8}$$

For flow through a porous medium, such as the pebble-bed, it has been found [14] that the convective terms and diffusive or shear stresses terms may be neglected if

$$\frac{|\vec{B}|L}{\rho\vec{V}\cdot\vec{V}}\gg 1\tag{9}$$

In the case of the pebble-bed reactor the dimensionless resistance force (9) due to the spheres is approximately 1470. The equation for the momentum in the radial direction may therefore be reduced to (assuming the y-direction to be the true vertical direction)

$$\varepsilon\rho\frac{\partial u_r}{\partial t}=-\varepsilon\frac{\rho V^2}{2T_o}\frac{\partial T_o}{\partial r}-\varepsilon\frac{p}{p_o}\frac{\partial p_o}{\partial r}-\varepsilon\rho g\frac{\partial y}{\partial r}-B_r\tag{10}$$

Similarly the equation for the momentum in the axial direction may be written as

$$\varepsilon\rho\frac{\partial u_z}{\partial t}=-\varepsilon\frac{\rho V^2}{2T_o}\frac{\partial T_o}{\partial z}-\varepsilon\frac{p}{p_o}\frac{\partial p_o}{\partial z}-\varepsilon\rho g\frac{\partial y}{\partial z}-B_z\tag{11}$$

Note, however, that part of the convective terms are retained through the total temperature and total pressure terms. It can be shown that the contribution of viscous dissipation is negligible compared to other the terms in the energy equation. The equation for the conservation of energy for the fluid in terms of the total specific enthalpy is then given as

$$\begin{aligned}\frac{\partial}{\partial t}(\varepsilon\rho h_o)+\frac{1}{r}\frac{\partial}{\partial r}(\varepsilon r\rho h_o u_r)+\frac{\partial}{\partial z}(\varepsilon\rho h_o u_z)\\ =\varepsilon\frac{\partial p}{\partial t}+\frac{1}{r}\frac{\partial}{\partial r}\left(\varepsilon rk\frac{\partial T}{\partial r}\right)+\frac{\partial}{\partial z}\left(\varepsilon k\frac{\partial T}{\partial z}\right)\\ +\varepsilon\rho(g_r u_r+g_z u_z)+q'''_{\mathrm{sf}}\end{aligned}\tag{12}$$

Solids and pebbles. In the case of the solids three energy equations can be distinguished, that is, the conduction in the reflector blocks, conduction in the pebbles and the heat transfer between the pebbles. The conservation equation in integral form for energy for the solids (excluding the pebbles) in the pebble-bed reactor can be written as [11,12]

$$\begin{aligned}\frac{\mathrm{d}}{\mathrm{d}t}\int_{\overline{V}}(1-\varepsilon)\rho_s e\,\mathrm{d}\overline{V}+\int_A(1-\varepsilon)\vec{n}\cdot\vec{q}\,\mathrm{d}A\\ =\int_{\overline{V}}(1-\varepsilon)\big(q'''_{\mathrm{fs}}+q'''_s\big)\,\mathrm{d}\overline{V}\end{aligned}\tag{13}$$

with $\vec{q}=-k_s\vec{\nabla}T$. The conservation equation in integral form for energy for the interior of a pebble can be written as [11]

$$\frac{\mathrm{d}}{\mathrm{d}t}\int_{\overline{V}}\rho_p e\,\mathrm{d}\overline{V}+\int_A\vec{n}\cdot\vec{q}\,\mathrm{d}A=\int_{\overline{V}}q'''_p\,\mathrm{d}\overline{V}\tag{14}$$

with $\vec{q}=-k_p\vec{\nabla}T$. The energy or heat transfer between the surfaces of adjacent pebbles due to contact, convection and radiation can, as a first approximation, be represented by a conservation equation. The conservation equation can be written as

$$\int_A\vec{n}\cdot\vec{q}_{\mathrm{eff}}\,\mathrm{d}A=0\tag{15}$$

with $\vec{q}_{\mathrm{eff}}=-k_{\mathrm{eff}}\vec{\nabla}T$.

Eqs. (13)–(15) can also be transformed into an equivalent set of partial differential equations through the divergence theorem. The equation for the conservation of energy in the solids can be written in axi-symmetric coordinates as

$$\begin{aligned}\frac{\partial}{\partial t}\big[(1-\varepsilon)\rho_s e\big]\\ =\frac{1}{r}\frac{\partial}{\partial r}\left\{(1-\varepsilon)r\left[k_s\frac{\partial T}{\partial r}\right]\right\}+\frac{\partial}{\partial z}\left\{(1-\varepsilon)\left[k_s\frac{\partial T}{\partial z}\right]\right\}\\ +(1-\varepsilon)\big(q'''_{\mathrm{fs}}+q'''_s\big)\end{aligned}\tag{16}$$

It is assumed that the temperature distribution in a pebble is the same in all radial directions. The equation for the conservation of energy in a pebble can therefore be written in one-dimensional spherical coordinates as

$$\frac{\partial}{\partial t}(\rho c_v T)=\frac{1}{r^2}\left[\frac{\partial}{\partial r}\left(k_p r^2\frac{\partial T}{\partial r}\right)\right]+q'''_p\tag{17}$$

Lastly the heat transfer between the surfaces of adjacent pebbles due to contact, convection and radiation can be written in axi-symmetric cylindrical coordinates as

$$0=\frac{1}{r}\frac{\partial}{\partial r}\left\{rk_{\mathrm{eff}}\frac{\partial T}{\partial r}\right\}+\frac{\partial}{\partial z}\left\{k_{\mathrm{eff}}\frac{\partial T}{\partial z}\right\}\tag{18}$$

Constitutive equations. The variation in the porosity in the radial direction due to the influence of the walls is taken into account by the correlation of Hunt and Tien [15]. The correlation was adapted for the annular configuration as follows

$$\varepsilon(r)=\varepsilon_b\left[1+\left(\frac{1-\varepsilon_b}{\varepsilon_b}\right)\exp\left(-6\cdot\frac{r-R_i}{d_p}\right)\right]\quad\text{for } R_i\leqslant r\leqslant\frac{R_o+R_i}{2}\tag{19}$$

and

$$\varepsilon(r)=\varepsilon_b\left[1+\left(\frac{1-\varepsilon_b}{\varepsilon_b}\right)\exp\left(-6\cdot\frac{R_o-r}{d_p}\right)\right]\quad\text{for } \frac{R_o+R_i}{2}\leqslant r\leqslant R_o\tag{20}$$

Because of the multi-dimensional nature of the flow patterns in the pebble-bed, the vectorial form of the Ergun equation

for the pebble-bed [16] has to be used as the constitutive equation for the resistance force $\vec{B}$ due to the pebbles in the momentum equations. Following Kuipers et al. [12] the resistance force due to the pebbles is therefore written as

$$\vec{B} = \left[\frac{160}{\rho d_p^2}\frac{(1-\varepsilon)^2}{\varepsilon^2} + 3|\vec{V}|\frac{(1-\varepsilon)^{1.1}}{\varepsilon\, d_p}\left(\frac{\mu}{\rho\varepsilon|\vec{V}|d_p}\right)^{0.1}\right]\rho\varepsilon\vec{V} = \varepsilon\beta\rho\vec{V} \tag{21}$$

The terms in Eqs. (10) and (11) due to the resistance of the spheres can therefore be written as $B_r = \varepsilon\rho\beta u_r$ and $B_z = \varepsilon\rho\beta u_z$ respectively.

The Zehner–Schlünder correlation with modifications similar to those used in the THERMIX code calculation [17] is employed to determine the effective conductivity k_{eff} for the heat transfer between the pebbles.

Integration of equations. Integrating Eqs. (10)–(12) for the fluid over a control volume leads to the following algebraic equations. Integrating the equation for the conservation of mass gives

$$\overline{V}_p\frac{\partial}{\partial t}(\varepsilon_p\rho_p) + (\varepsilon\rho u_r)_e A_e - (\varepsilon\rho u_r)_w A_w + (\varepsilon\rho u_z)_n A_n - (\varepsilon\rho u_z)_s A_s = 0 \tag{22}$$

The integration of the equation for the conservation of momentum in the radial direction gives

$$\begin{aligned}\varepsilon_p\rho_p\bar{A}_r\Delta r\frac{\partial(u_r)_p}{\partial t} &= -\varepsilon_p\frac{\rho_p V_p^2}{2(T_o)_p}\bar{A}_r\big[(T_o)_e - (T_o)_w\big] - \varepsilon_p\frac{p_p}{(p_o)_p}\bar{A}_r\big[(p_o)_e - (p_o)_w\big]\\ &\quad - \varepsilon_p\rho_p g\bar{A}_r[y_e - y_w] - \varepsilon_p\rho_p\beta(u_r)_p\bar{A}_r\Delta r\end{aligned} \tag{23}$$

while the integration of the equation for the conservation of momentum in the axial direction results in

$$\begin{aligned}\varepsilon_p\rho_p\bar{A}_z\Delta z\left(\frac{\partial u_z}{\partial t}\right)_p &= -\varepsilon_p\frac{\rho_p V_p^2}{2(T_o)_p}\bar{A}_z\big[(T_o)_n - (T_o)_s\big] - \varepsilon_p\left(\frac{p}{p_o}\right)_p\bar{A}_z\big[(p_o)_n - (p_o)_s\big]\\ &\quad - \varepsilon_p\rho_p g\bar{A}_z[y_n - y_s] - \varepsilon_p\rho_p\beta(u_z)_p\bar{A}_z\Delta z\end{aligned} \tag{24}$$

The integration of the equation for the conservation of energy for the fluid gives

$$\begin{aligned}&\overline{V}_p\frac{\partial}{\partial t}\big[\varepsilon_p\rho_p(h_o)_p\big] + (\varepsilon\rho h_o u_r)_e A_e - (\varepsilon\rho h_o u_r)_w A_w + (\varepsilon\rho h_o u_z)_n A_n - (\varepsilon\rho h_o u_z)_s A_s\\ &= \overline{V}_p\left(\varepsilon\frac{\partial p}{\partial t}\right)_p + \left(\varepsilon k\frac{\partial T}{\partial r}\right)_e A_e - \left(\varepsilon k\frac{\partial T}{\partial r}\right)_w A_w + \left(\varepsilon k\frac{\partial T}{\partial z}\right)_n A_n - \left(\varepsilon k\frac{\partial T}{\partial z}\right)_s A_s\\ &\quad + \varepsilon_p\rho_p(g_r u_r + g_z u_z)_p\overline{V}_p + q'''_{\text{sf}}\overline{V}_p\end{aligned} \tag{25}$$

Integrating Eqs. (16)–(18) for the solids and the pebbles also leads to the following algebraic equations. The equation for the conservation of energy for the solids gives

$$\begin{aligned}&\overline{V}_p\frac{\partial}{\partial t}\big[(1-\varepsilon)\rho e\big]_p\\ &= \left\{(1-\varepsilon)\left[k_s\frac{\partial T}{\partial r}\right]\right\}_e A_e - \left\{(1-\varepsilon)\left[k_s\frac{\partial T}{\partial r}\right]\right\}_w A_w + \left\{(1-\varepsilon)\left[k_s\frac{\partial T}{\partial z}\right]\right\}_n A_n - \left\{(1-\varepsilon)\left[k_s\frac{\partial T}{\partial z}\right]\right\}_s A_s\\ &\quad + (1-\varepsilon_p)\big(q'''_{\text{fs}} + q'''_s\big)\overline{V}_p\end{aligned} \tag{26}$$

The integration of the equation for the conservation of energy for a pebble results in

$$\overline{V}_p\frac{\partial}{\partial t}[\rho_p e]_p = \left[k_p\frac{\partial T}{\partial r}\right]_e A_e - \left[k_p\frac{\partial T}{\partial r}\right]_w A_w + q'''_p\overline{V}_p \tag{27}$$

and finally the equation for the transfer of heat between adjacent pebbles becomes

$$\left[k_{\text{eff}}\frac{\partial T}{\partial r}\right]_e A_e - \left[k_{\text{eff}}\frac{\partial T}{\partial r}\right]_w A_w + \left[k_{\text{eff}}\frac{\partial T}{\partial z}\right]_n A_n - \left[k_{\text{eff}}\frac{\partial T}{\partial z}\right]_s A_s = 0 \tag{28}$$

Heat transfer correlations. For the heat transfer at the interfaces between the fluid and the solids or pebbles the applicable boundary terms or source terms in Eqs. (25)–(27) are replaced with the appropriate correlations.

The pebbles in the packed-bed can be considered as heat exchangers each with a constant surface temperature. This type of heat exchanger can be modelled with the aid of the effectiveness-NTU method. The heat transfer rate q_{pf} between a pebble and the fluid is given as

$$q_{\text{pf}} = -k_p A\frac{\partial T}{\partial n}\bigg|_s = kA\frac{\partial T}{\partial n}\bigg|_f = -\epsilon|\dot{m}_p c_p|(T_f - T_s) \tag{29}$$

The heat transfer coefficient required in the calculation is determined from the correlation for the Nusselt number proposed by Kugeler and Schulten [16].

2.3. Discretization

A study of Eqs. (22)–(29) reveal that they are one-dimensional, or can be written as the sum of two one-dimensional equations. This formulation of the equations allows the pebble bed reactor to be discretized into a collection of one-dimensional elements (models) that can be incorporated with ease in a general systems CFD approach [10]. Fig. 2 shows a simplified network representation of the solids in the pebble-bed and core structures of Fig. 1. In the network both the pebble-bed and the core

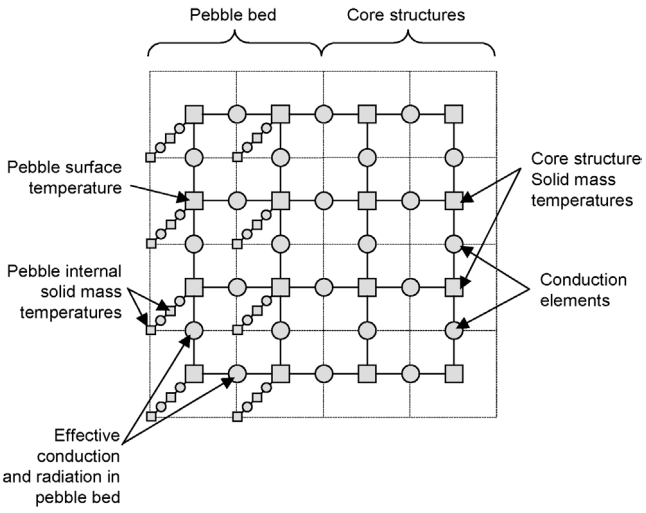

Fig. 2. Simplified network representation of solids in pebble-bed and core structures.

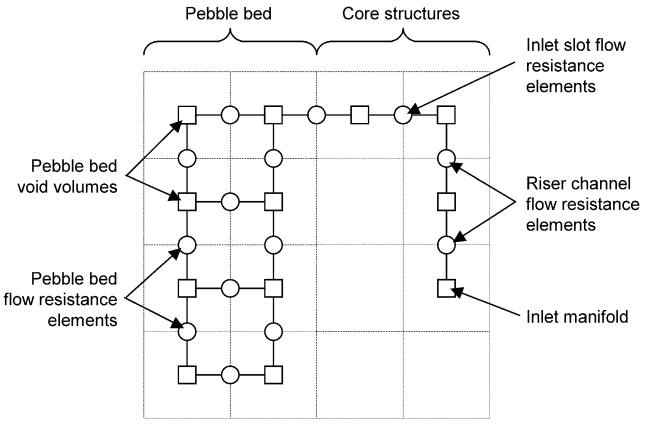

Fig. 3. Simplified network representation of the riser channels, inlet slots and packed-bed flow path within the pebble-bed and core structures.

structures are represented by two control volumes in the radial direction and four control volumes in the axial direction. In the case of the core structures, the large light grey squares (nodes) represent the mass of the solid material and therefore also the temperatures of the core structure material that is assumed to be homogeneous throughout a control volume. The large grey circles (elements) represent the radial and axial conduction respectively within the core structures. In the case of the pebble-bed, the large grey squares represent only the outer layer of the pebbles in that control volume and therefore also the surface temperature of all the pebbles in that specific control volume. The inner layers of the solid mass of a pebble is represented by the smaller grey squares. It will therefore be possible to calculate a temperature distribution profile within the pebbles of each control volume. The small grey circles represent the one-dimensional spherical heat conduction within the pebble while the large grey circles represent the effective conduction and radiation between the pebble surfaces within the bed.

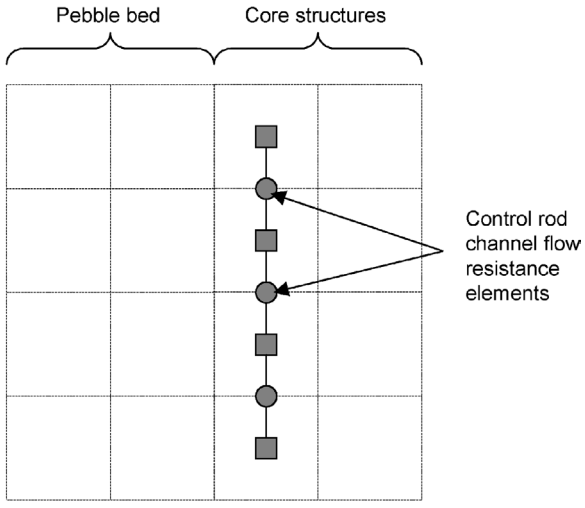

Fig. 4. Simplified network representation of the control rod channels flow path within the core structures.

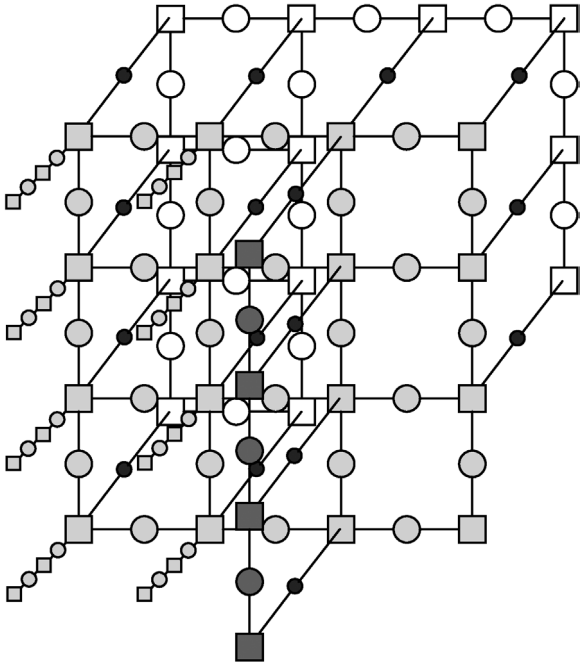

Fig. 5. Integrated network representation of the pebble-bed and core structures solids and flow paths.

Fig. 3 shows a simplified network representation of the riser channel, inlet slots and packed-bed flow path within the pebble bed and core structures of Fig. 1. In Fig. 3 the white squares represent the void gas volumes and the circles the flow resistance elements. The node on the bottom right also represents the inlet manifold in which the gas is assumed to be well-mixed so that a homogeneous temperature will be obtained.

As noted earlier, the gas flowing in the riser channels, inlet slots and through the pebble bed does not mix with the gas flowing in the control rod channels. This means that a second, separated gas flow network is required to simulate

the flow in the control rod channels. This network is shown in Fig. 4 as dark grey nodes and elements.

The interaction between the solid structure network and the respective flow networks is via fluid/solid surface convection. This interaction is shown schematically in Fig. 5. In the figure the surface convection elements are shown in black, the control rod channel flow network in dark grey, the solid network in light grey and the riser channels, inlet slots and pebble bed flow path in white.

Fig. 5 highlights one of the distinct advantages of employing the network approach rather than the traditional CFD approach. That is that even though the simplifying assumption was made earlier of two-dimensional axisymmetric geometry, both of the riser channel and control rod channel flow paths that is unmixed, can be simulated together with its interaction with the solid structures. This is done by simply superimposing another network layer and adding the correct connectivity via surface convection elements.

3. Results

Having developed the theoretical basis for the new systems CFD model, it is important to prove its validity by comparing the numerical results with that of experiments.

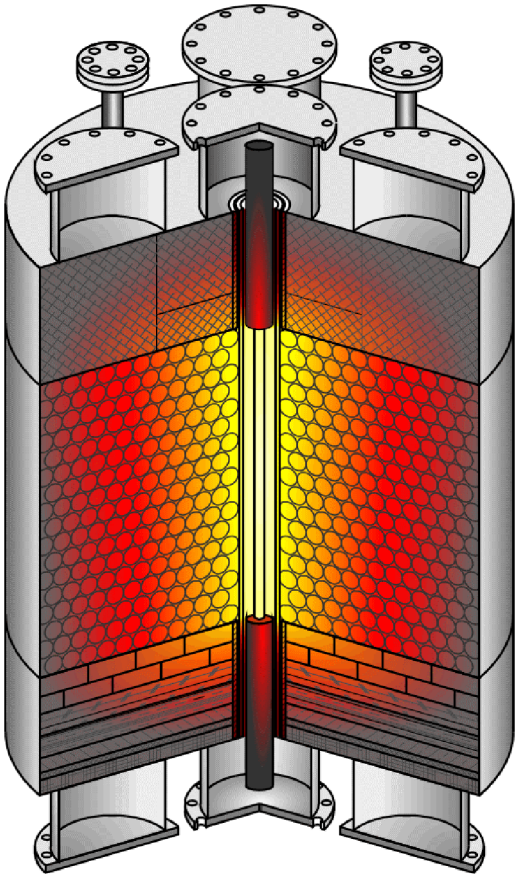

Fig. 6. Schematic of SANA test facility taken from [18].

Of particular importance is the prediction of the pebble temperatures obtained in the case of natural convection driven flows that will prevail after critical pressurized or depressurized loss of forced cooling events. Fortunately suitable data does exist in the form of the experimental results obtained from the SANA test facility [18]. The SANA test facility was installed at the Research Centre Jülich in Germany specifically to investigate the heat transport mechanisms inside the core of a high temperature gas cooled reactor (HTGR).

3.1. SANA test facility

The test facility consisted of a heated pebble bed inside a furnace to simulate the thermal conditions of such a HTGR-core. Different heater configurations were possible but Fig. 6 shows a schematic of the test facility with a single central heating element. The diameter of the pebble bed is 1.5 m and the height is 1.0 m. The overall height of the facility is 3.2 m and the maximum heating capacity of the single central heating element is 35 kW. The top and bottom of the facility was well-insulated while the outside of the furnace was open to atmosphere. More than 50 steady-state as well as various transient tests were carried out on the facility. In

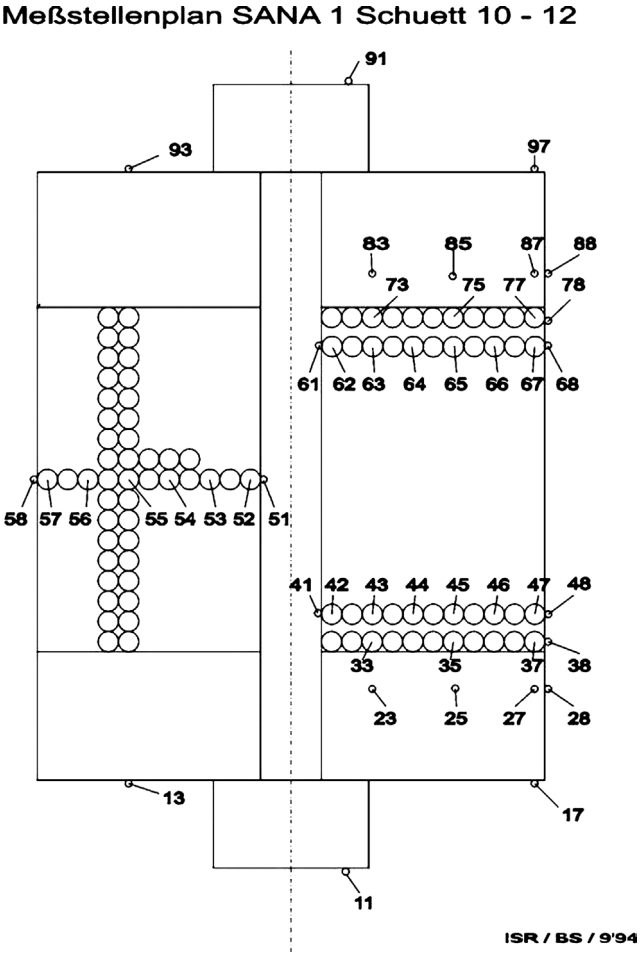

Fig. 7. Schematic of the temperature measuring points on the SANA test facility taken from [18].

these experiments all the main parameters of a pebble bed were varied, such as pebble material, pebble diameter, gas, heating power and heating geometry.

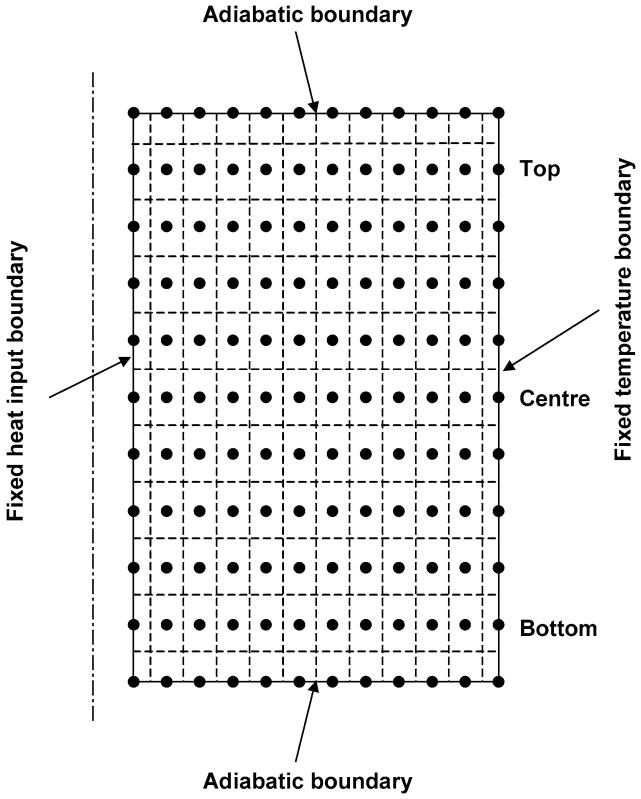

Fig. 8. Schematic of the discretization scheme used in all of the Flownex simulations.

For the tests conducted with the 60 mm diameter graphite pebbles, measurements were taken of the pebble temperatures at different radial positions close to the bottom of the pebble bed (height 90 mm) as well as at the center (height 500 mm) and top (height 910 mm) as shown in Fig. 7. Detailed results of these tests are presented in [18].

3.2. Comparison between Flownex and SANA results

This section will present comparisons between results produced by Flownex and results obtained with SANA for six cases. In all six cases the furnace contained graphite pebbles with 60 mm diameter, which is naturally of particular interest to the PBMR application. The cases are limited to steady-state conditions (transient results will be presented at a later stage), but cover the whole range of temperatures between 60 °C and 1150 °C. It also includes two fluids with very different natural convection properties, i.e., helium and nitrogen, and also different heating configurations.

In all of the simulations the pebble bed was discretised into control volumes with equal heights and equal radial widths. Half control volumes were employed at all the boundaries as shown in Fig. 8. The bottom and top boundaries were assumed to be adiabatic and no allowance was made for conductive heat transfer within the material situated at the inner and outer boundaries of the pebble bed. The outer wall temperatures measured for the respective experiments were applied to the outer boundary while the heat input to the heating element was distributed uniformly at the inner boundary.

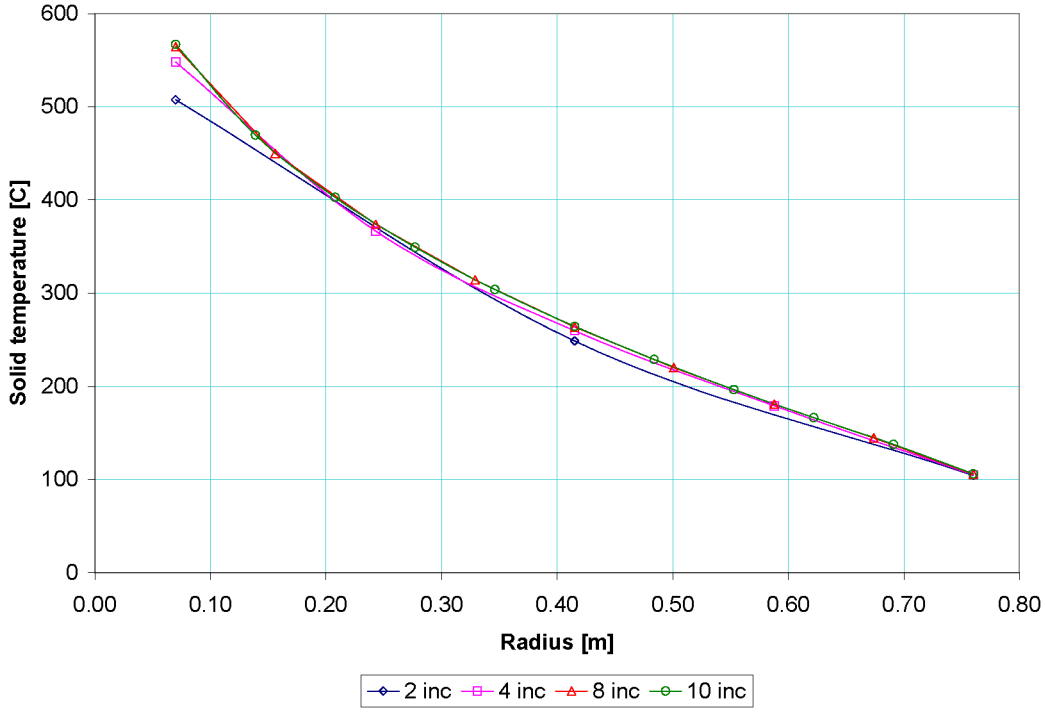

Fig. 9. Pebble temperatures for Helium with 10 kW steady-state power input for two, four, eight and ten increments in the radial and axial directions.

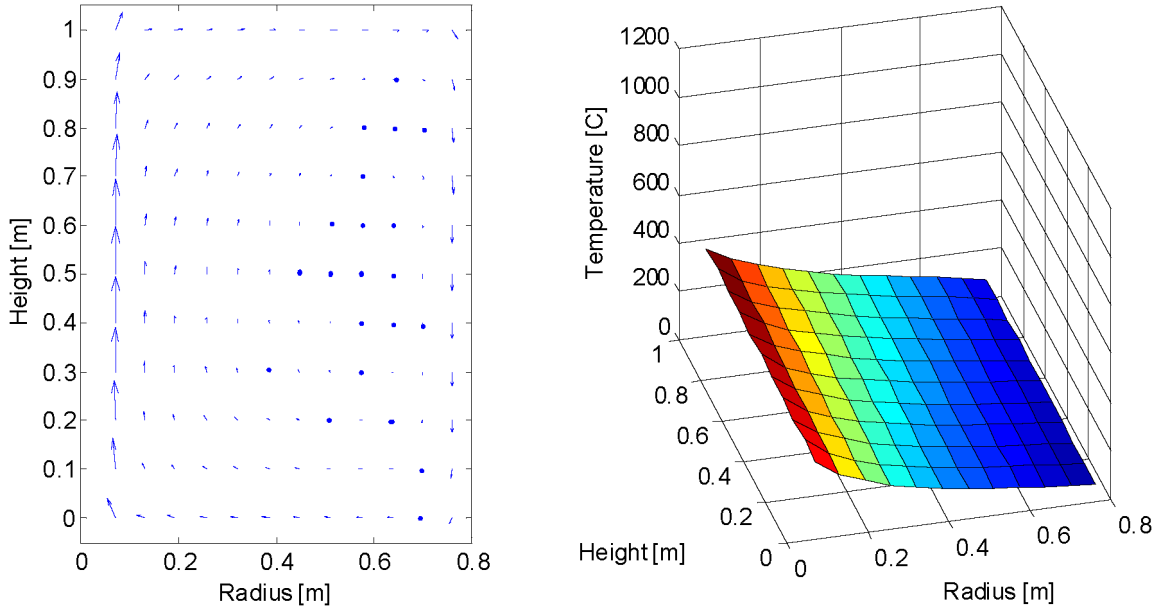

Fig. 10. Velocity and temperature distributions for Helium with 5 kW nominal heating power along the full height of the pebble bed.

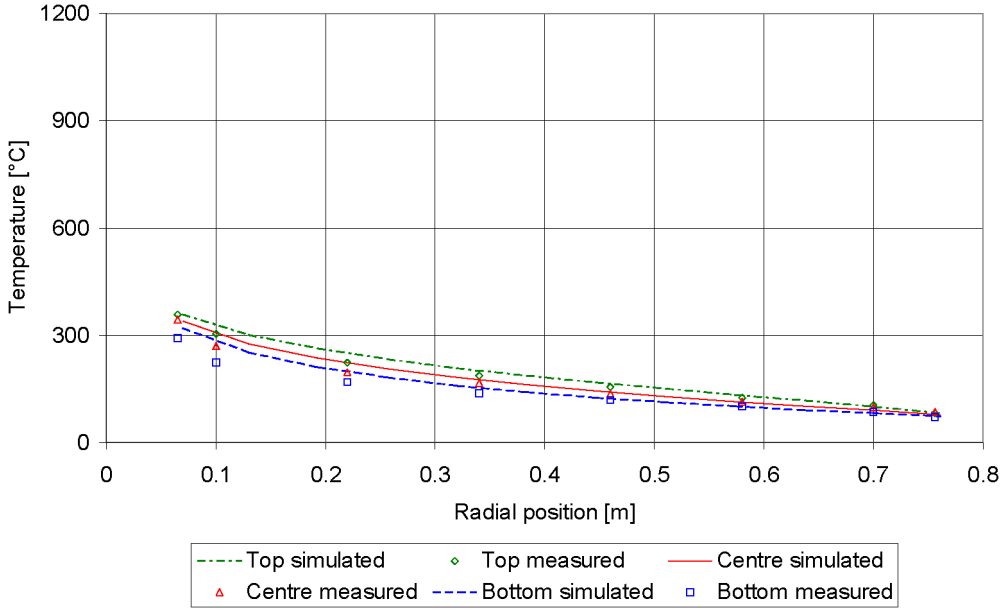

Fig. 11. Results of measured (SANA) and simulated (Flownex) pebble temperatures for Helium with 5 kW nominal heating power along the full height of the pebble bed.

A grid dependence study was conducted prior to fixing the size of the control volumes. The study compared the predicted temperature distribution in the pebbles along the radial direction at the centre of the pebble bed for steady-state conditions. The test case employed Helium as working fluid and 10 kW of heat input at the central heating element. For the test case an equal number of radial and axial increments of two, four, eight and ten respectively were used. From the results shown in Fig. 9 it is clear that there is very little difference between the results obtained for eight and ten increments, suggesting that a grid-independent solution is obtained with as little as eight increments. Given this, and for the sake of convenient comparison with the measured data, ten equal height increments of 100 mm each and 23 equal width radial increments of 29.6 mm each were used in all the subsequent simulations.

The computer simulation time for each of the six simulations was less than three seconds per run on a notebook computer with a 1.6 GHz Centrino processor and 512 Megabytes of memory.

Case 1. The first case that will be considered is Helium with 5 kW nominal heating power along the full height of the pebble bed. Fig. 10 shows the velocity vectors and tempera-

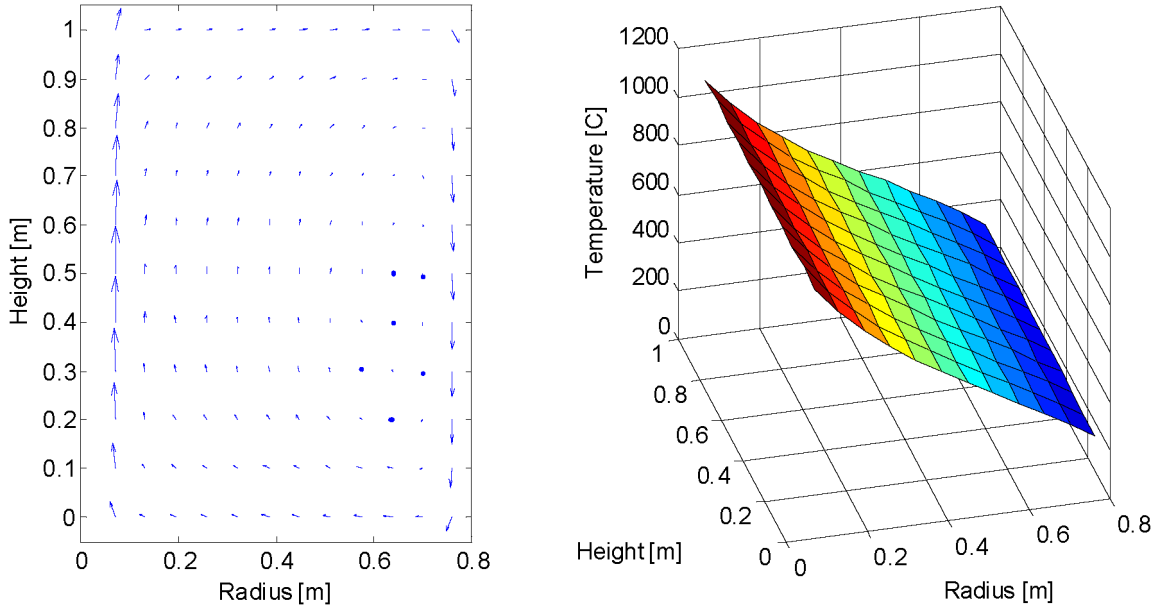

Fig. 12. Velocity and temperature distributions for Helium with 35 kW nominal heating power along the full height of the pebble bed.

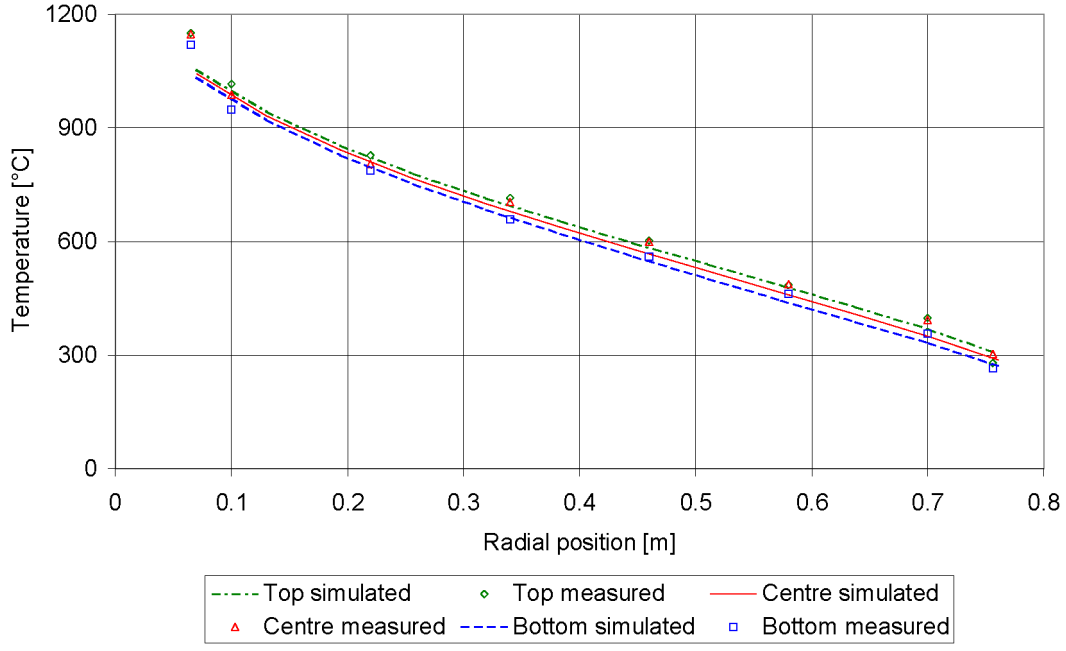

Fig. 13. Results of measured (SANA) and simulated (Flownex) pebble temperatures for Helium with 35 kW nominal heating power along the full height of the pebble bed.

ture distribution for the flow field, whilst Fig. 11 shows the comparison between the measured (SANA) and simulated (Flownex) temperatures for this case at the top, center and bottom of the pebble bed.

Case 2. The second case is also Helium but with 35 kW nominal heating power along the full height of pebble bed. Fig. 12 shows the velocity vectors and temperature distribution for the flow field, Fig. 13 shows the comparison between the measured and simulated temperatures for this case.

The flow fields shown in Figs. 10 and 12 are typical of buoyancy driven flow in an annular cavity with a heated inner wall and the small temperature gradient in the axial direction in both cases is indicative of the high thermal conductivity of Helium. The effect of the higher heating power on the temperature variation in the radial direction can also be observed. Figs. 11 and 13 show that good agreement is obtained between the SANA and Flownex results for Helium over the full range of temperatures, although there is some deviation at the inner boundary for the 35 kW case. This can most probably be attributed to the fact that the model for the

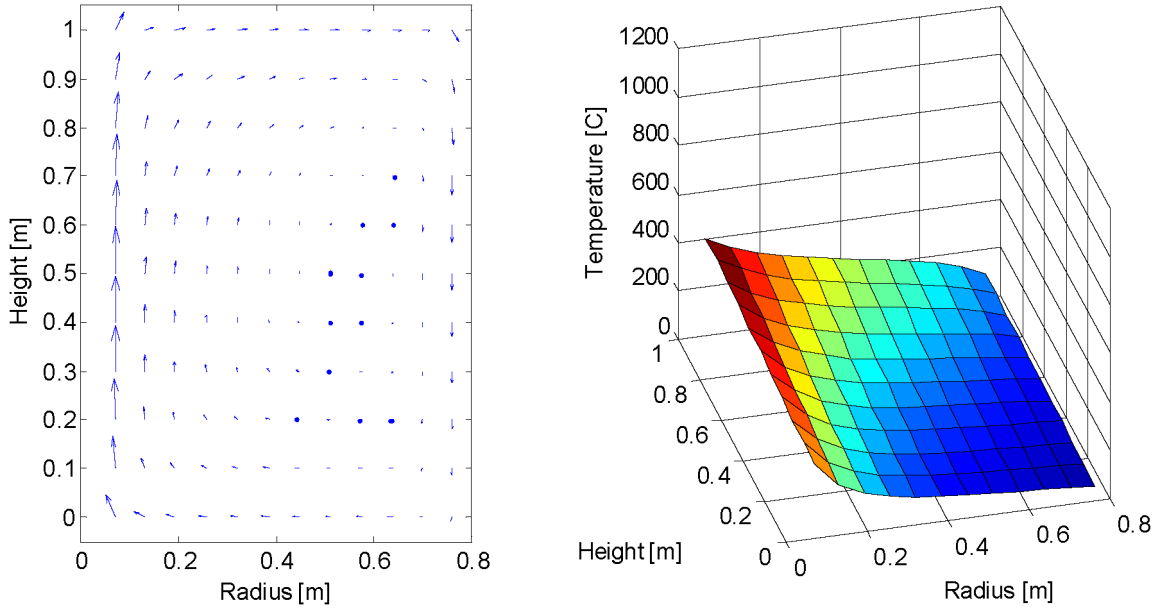

Fig. 14. Velocity and temperature distributions for Nitrogen with 5 kW nominal heating power along the full height of the pebble bed.

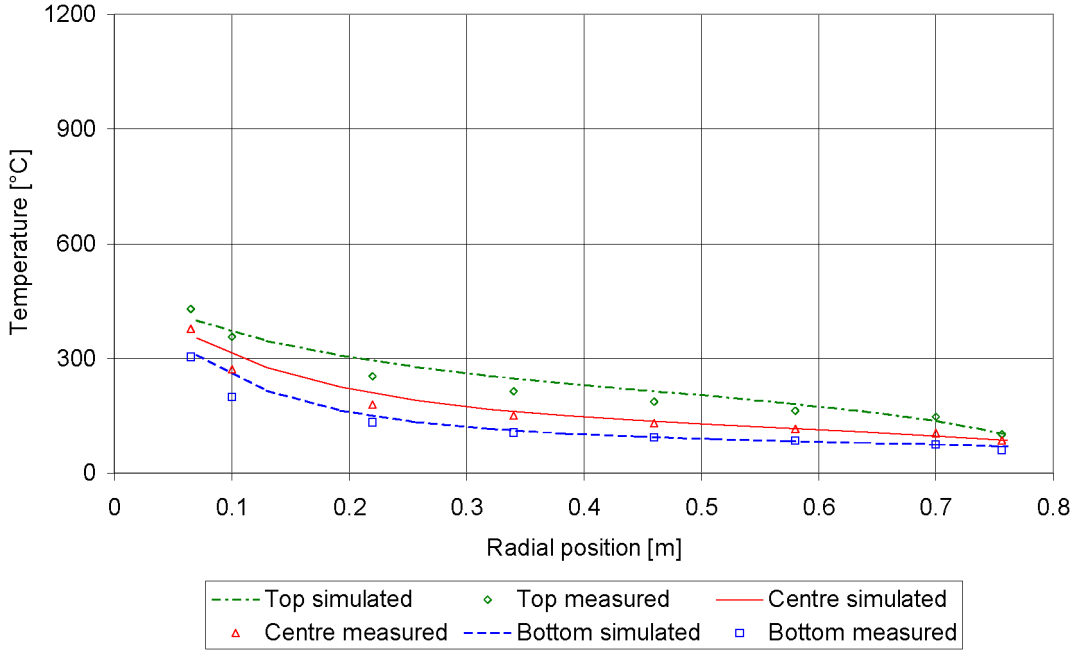

Fig. 15. Results of measured (SANA) and simulated (Flownex) pebble temperatures for Nitrogen with 5 kW nominal heating power along the full height of the pebble bed.

effective conductivity currently does not distinguish between the phenomena within the bed where heat is transferred between pebble surfaces and the phenomena at the edge of the pebble bed where heat is transferred between the pebble and the side-wall surfaces.

Case 3. Fig. 14 shows the velocity vectors and temperature distribution for the flow field, whilst Fig. 15 shows the comparison between the measured and simulated temperatures for Nitrogen with 5 kW nominal heating power along the full height of pebble bed.

Case 4. Case 4 is again for Nitrogen but with 35 kW nominal heating power along the full height of pebble bed. Fig. 16 shows the velocity vectors and temperature distribution for the flow field, whilst Fig. 17 shows the comparison between the measured and simulated temperatures.

Also in these cases the flow fields shown in Figs. 14 and 16 are typical of buoyancy driven flow in annular cavity with a heated inner wall. The larger temperature gradient in the axial direction, compared to that in Figs. 10 and 12,

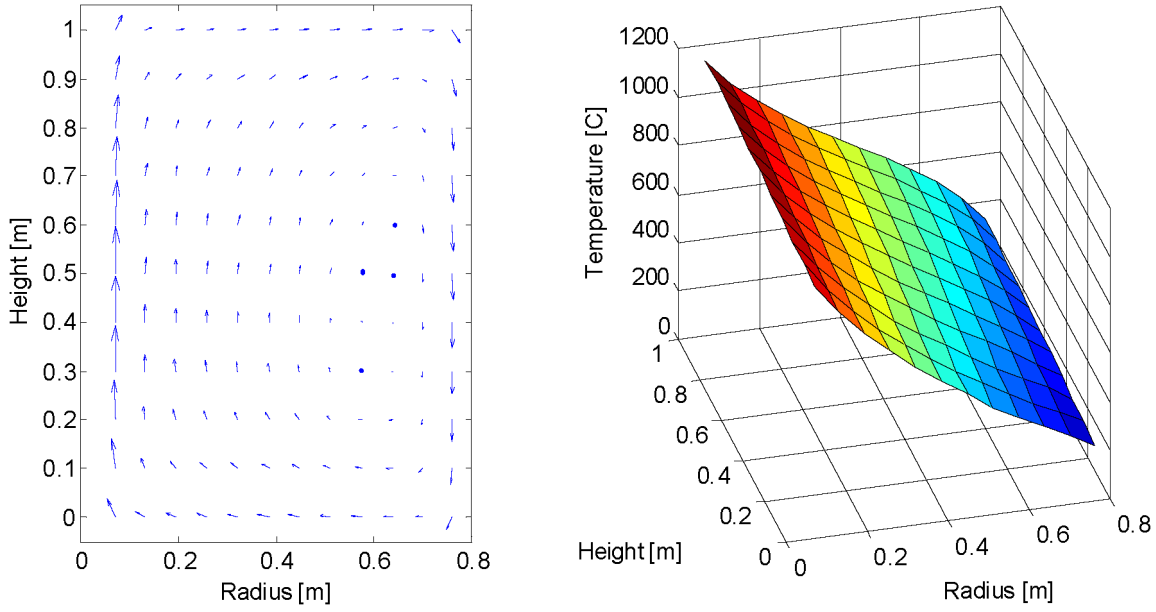

Fig. 16. Velocity and temperature distributions for Nitrogen with 35 kW nominal heating power along the full height of the pebble bed.

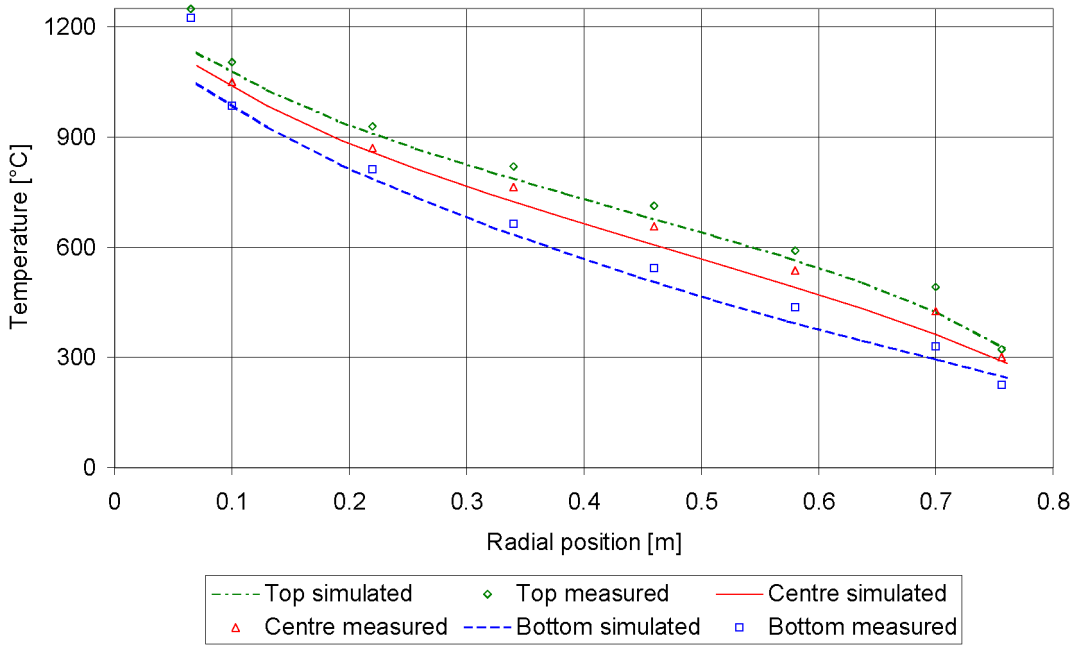

Fig. 17. Results of measured (SANA) and simulated (Flownex) pebble temperatures for Nitrogen with 35 kW nominal heating power along the full height of the pebble bed.

is indicative of the poorer thermal conductivity of Nitrogen. Again the effect of the higher heating power on the temperature variation in the radial direction can be observed. From Figs. 15 and 17 it is clear that good agreement is also obtained between the SANA and Flownex results for Nitrogen over the full range of temperatures. There is however again some deviation at the inner boundary for the 35 kW case. From the figures it is also evident that the natural convection phenomena are much more significant in the case of Nitrogen than in the case of Helium, resulting in much more prominent temperature stratification.

The next two cases are both for Nitrogen with a nominal heat input of 20 kW. However, the heating will not take place along the full length of the pebble bed. The first case will only have heating in the top half of the bed while the second case will only have heating in the bottom half of the bed.

Case 5. Fig. 18 shows the velocity vectors and the temperature distribution, whilst Fig. 19 shows the comparison between the measured and simulated temperatures for this case where the heating is only distributed in the top half of the pebble bed.

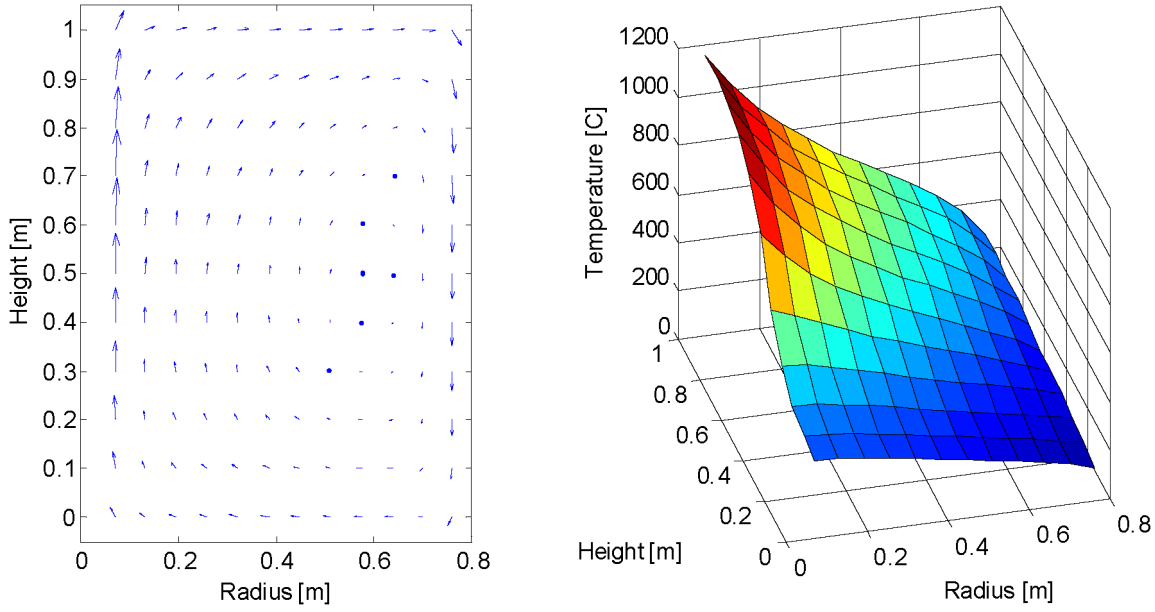

Fig. 18. Velocity and temperature distributions for Nitrogen with 20 kW nominal heating power in the top half of the pebble bed only.

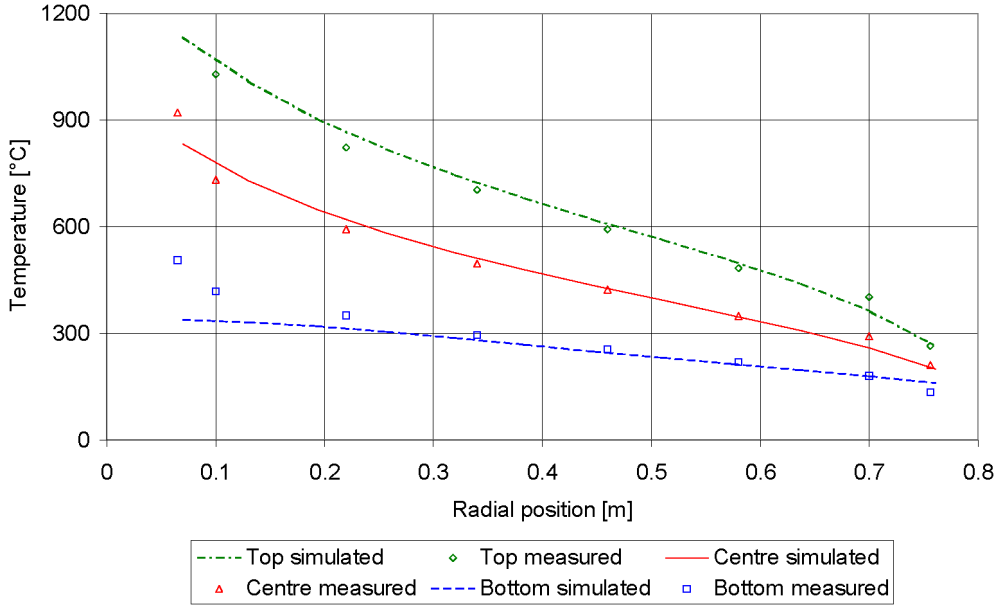

Fig. 19. Results of measured (SANA) and simulated (Flownex) pebble temperatures for Nitrogen with 20 kW nominal heating power in the top half of the pebble bed only.

The results clearly show the effect on the flow field of the concentrated heating that results in much higher temperatures in the top half of the pebble bed. Once again, the simulated temperatures at the inner boundary are lower than the measured values. This difference is more pronounced in the bottom part of the bed. In this case it may also be due in part to the fact that in the experiment there is heat conduction from the top to the bottom of the sheath surrounding the heating element that is situated at the inner boundary of the bed, thus heating the bottom half of the inner wall. In the case of the simulation model, no allowance was made for this longitudinal heat conduction. However, good agreement is again obtained between the SANA and Flownex results.

Case 6. Case 6 is Nitrogen with 20 kW nominal heating power that is only distributed in the bottom half of the pebble bed. Fig. 20 shows the velocity vectors and the temperature distribution and Fig. 21 shows the comparison between the measured and simulated temperatures for this case at the top, center and bottom of the pebble bed.

The results of the simulation again agree well with that of the experiment with some deviation at the inner bound-

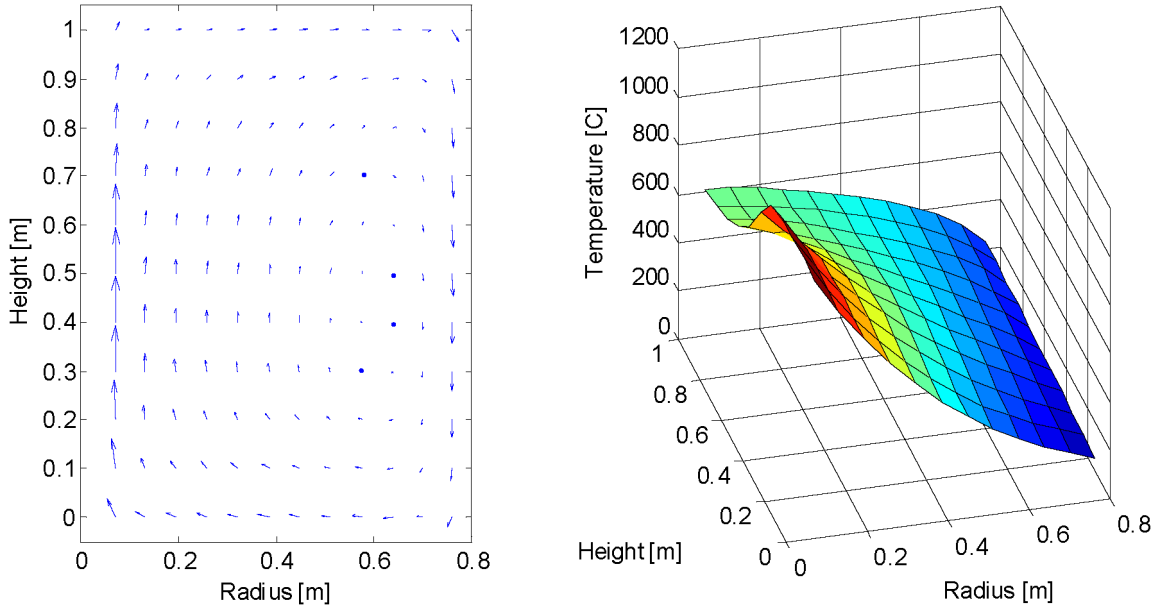

Fig. 20. Velocity and temperature distributions for Nitrogen with 20 kW nominal heating power in the bottom half of the pebble bed only.

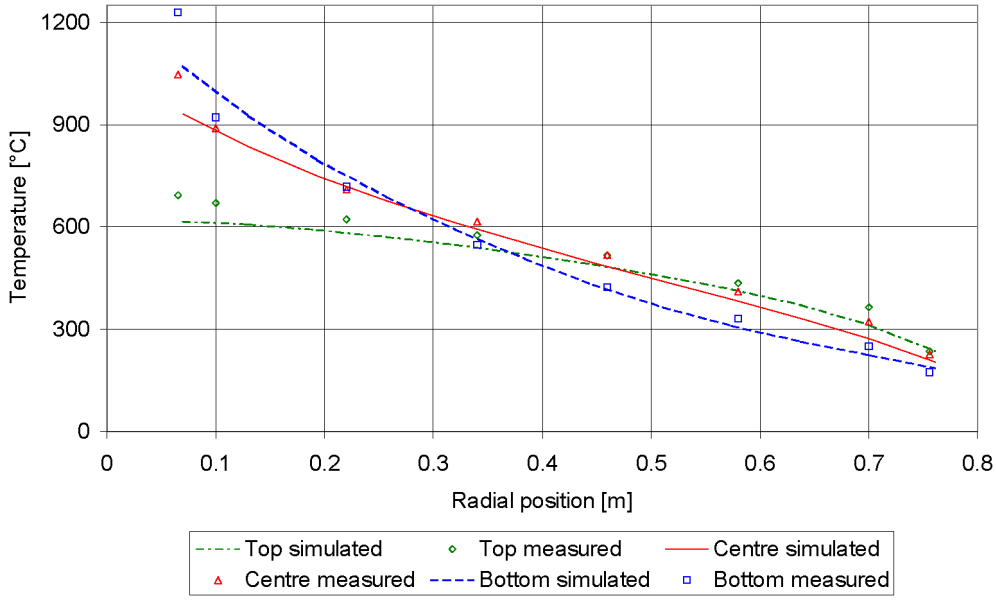

Fig. 21. Results of measured (SANA) and simulated (Flownex) pebble temperatures for Nitrogen with 20 kW nominal heating power in the bottom half of the pebble bed only.

ary. The temperature distribution shown in Fig. 21 provides valuable insight into the trends observed in Fig. 21. The simulation model also clearly accounts well for the effect of the heating that only takes place in the bottom half of the bed. It shows that although natural convection phenomena are present, much of the heat generated at the bottom inner boundary of the bed is transported in the radial direction without being transported to the upper part of the inner boundary. However, the increased natural convection ensures that the heat is well dispersed from the average radius onwards.

4. Conclusions

The theoretical basis and conceptual formulation of a comprehensive reactor model to simulate the thermal-fluid phenomena of the PBMR reactor core and core structures was given. Through a rigorous analysis the fundamental equations were recast in a form that is suitable for incorporation in a systems CFD code. The formulation of the equations resulted in a collection of one-dimensional elements (models) that can be used to construct a comprehensive multi-dimensional network model of the reactor. The

good comparison obtained between the simulated and measured results for all six of the cases presented shows that the systems CFD approach sufficiently accounts for all of the important phenomena encountered in the quasi-steady natural convection driven flows that will prevail after critical events in a reactor. The fact that the computer simulation time for all of the simulations was less than three seconds on a standard notebook computer also indicates that the new model indeed achieves a fine balance between accuracy and simplicity. The new model can therefore be used with confidence and still allow quick integrated plant simulations.

Acknowledgements

The authors wish to thank PBMR (Pty) Ltd. whose financial support made this work possible as well as M-Tech Industrial (Pty) Ltd., developers of the Flownex software.

References

[1] PBMR (Pty) Ltd. Reactor Safety Analysis Report of the South-African Pebble-Bed Modular Reactor (PBMR), Rev. E, Centurion, South Africa.
[2] S. Becker, E. Laurien, Three-dimensional numerical simulation of flow and heat transport in high-temperature nuclear reactors, Nuclear Engrg. Design 222 (2003) 189–201.
[3] P.G. Rousseau, G.P. Greyvenstein, One-dimensional reactor model for the integrated simulation of the PBMR power plant, in: J.P. Meyer (Ed.), Proceedings of 1st Int. Conf. on Heat Transfer, Fluid Mechanics and Thermodynamics, Kruger Park, South Africa, 2002.
[4] M.P. Van Staden, C. Janse Van Rensburg, C.F. Viljoen, CFD simulation of helium gas cooled pebble bed reactor, in: J.P. Meyer (Ed.), Proceedings of 1st Int. Conf. on Heat Transfer, Fluid Mechanics and Thermodynamics, Kruger Park, South Africa, 2002.
[5] E.C. Verkerk, Dynamics of the pebble-bed nuclear reactor in the direct Brayton cycle, PhD thesis, Delft University of Technology, Delft, 2000.
[6] M.M. Stempniewicz, Steady-state and accident analyses of PBMR with the computer code SPECTRA, in: Trans. 1st Int. Topical Meeting on High Temperature Reactor Technology, Petten, Netherlands, 2002.
[7] J.F. Kikstra, Modelling, design and control of a cogeneration nuclear gas turbine plant, PhD thesis, Delft University of Technology, Delft, 2001.
[8] J. Van der Merwe, J.P. Van Ravenswaay, Flownex Version 6.4 User Manual, M-Tech Industrial, Potchefstroom, South Africa, 2003.
[9] G.P. Greyvenstein, P.G. Rousseau, Basic principles of HTR thermal-hydraulics, HTR/ECS 2002 High Temperature Reactor School, Cadarache, France, 2002.
[10] G.P. Greyvenstein, An implicit method for the analysis of transient flows in pipe networks, Int. J. Numer. Methods Engrg. 53 (2002) 1127–1143.
[11] R. Peyret, T.D. Taylor, Computational Methods for Fluid Flow, Springer, New York, 1983.
[12] J.A.M. Kuipers, K.J. Van Duin, F.P.H. Van Beckum, W.P.M. Van Swaaij, A numerical model of gas-fluidized beds, Chem. Engrg. Sci. 47 (1992) 1913–1924.
[13] O. Bey, G. Eigenberger, Fluid flow through catalyst filled tubes, Chem. Engrg. Sci. 52 (8) (1997) 1365–1376.
[14] STAR-CD Methodology Manual Version 3.10, Computational Dynamics, London, 2000.
[15] M.L. Hunt, C.L. Tien, Non-Darcian flow, heat and mass transfer in catalytic packed-bed reactors, Chem. Engrg. Sci. 45 (1990) 55–63.
[16] K. Kugeler, R. Schulten, Hochtemperaturreaktortechnik, Springer, Berlin, 1989.
[17] International Atomic Energy Agency, Heat transport and afterheat removal for gas cooled reactors under accident conditions, IAEA-TECDOC-1163, 2001.
[18] H.-F. Niessen, B. Stöcker, Data sets of SANA experiment: 1994–1996, JUEL-3409, Forschungszentrum Jülich, 1997.